Published by IOP Publishing for SISSA
Received: *November 20, 2008*
Accepted: *November 21, 2008*
Published: *December 3, 2008*

Leptogenesis with composite neutrinos

Yuval Grossman and Yuhsin Tsai

Institute for High Energy Phenomenology,
Newman Laboratory of Elementary Particle Physics
Cornell University, Ithaca, NY 14853, U.S.A.
E-mail: yuvalg@lepp.cornell.edu, yt237@lepp.cornell.edu

Abstract: Models with composite singlet neutrinos can give small Majorana or Dirac masses to the active neutrinos. The mechanism is based on the fact that conserved chiral symmetries give massless neutrinos at the renormalizable level. Thus, they acquire very small masses due to non-renormalizable terms. We investigate such models in two aspects. First, we find UV completions for them and then we investigate the possibility of giving leptogenesis. We find that these models offer new possibilities for leptogenesis. Models with Majorana masses can exhibit standard leptogenesis. Models with Dirac masses can provide a realization of Dirac type leptogenesis with mass scale that can be as low as 10 TeV.

Keywords: Neutrino Physics, Technicolor and Composite Models.

JHEP12(2008)016

Contents

JHEP12(2008)016

1. Introduction

In recent years it has become clear that neutrinos have very small masses and that they mix. The origin of these masses is still an open question. The see-saw mechanism is probably the most elegant explanation for small neutrino masses. The idea is to add heavy Majorana right handed (RH) neutrinos to the theory. These added particles give very small Majorana masses to the active, Standard Model (SM) neutrinos. The see-saw mechanism has one more virtue: it provides an elegant mechanism to explain the observed baryon asymmetry in the universe. The idea of this mechanism, called Leptogenesis (LG) [1], is that the heavy RH neutrinos that drive the see-saw also generate lepton asymmetry when they decay. Part of this lepton asymmetry is transformed into the observed baryon asymmetry of the universe (for a review see [2]).

While the see-saw mechanism is very simple and successful, it is not the only way to explain the observed small neutrino masses. Another idea for getting light neutrinos that has not been widely discussed is that of composite RH neutrinos [3, 4]. The basic idea is that there exists a new sector with strong dynamics at a scale Λ. The confinement in this sector leaves some chiral symmetries exact and produces massless composite fermions.

The only interaction between the preons of the new sector and the SM sector is via heavy messengers with large masses of order M. Then, the Yukawa coupling between the LH and RH neutrinos is suppressed by powers of the small factor Λ/M. This can give a natural explanation for small Dirac or Majorana neutrino masses.

In this article we further investigate the composite RH neutrino idea. First, we find UV completions for models that give Dirac or Majorana neutrino masses. We then study how these full models can give LG. We find that it exhibits interesting LG possibilities. In particular, it can have see-saw like LG and a low mass scale Dirac LG.

In the next section, we give a brief review of the composite RH neutrino idea of ref. [3]. We find UV complete theories in section III for both Dirac and Majorana neutrinos where the new particle content is given, and the experimental constraints are discussed. In section IV, we study LG possibilities in the model. When the temperature T is below the confinement scale, $T \ll \Lambda$, and the RH neutrinos are heavy, the composite structure of the RH neutrinos cannot be probed and standard LG become possible (IV.A). When $T \sim M \gg \Lambda$, the preons are asymptotically free and standard LG cannot work. In the case of Dirac neutrinos, the decay of heavy messengers gives a realization of a low energy Dirac LG (IV.B). In section V we conclude. A detailed calculation of the effective couplings is given in appendix A. The experimental bounds on the masses and couplings of the new fields arising from lepton flavor violating processes are given in appendices B and C.

2. Composite right-handed neutrino

We first review the idea of composite right-handed neutrinos [3]. Consider a new strong sector such that all the new fields are SM singlets. Like QCD, where the interaction becomes strong at a scale $\Lambda_{\rm QCD}$, the new sector becomes strong at a new scale Λ. Unlike QCD, however, we assume that the confinement in the new sector keeps some of the chiral symmetries unbroken. In that case, massless composite fermions are generated since they are required for anomaly matching of the unbroken chiral symmetries.

The view point in [3] is that of an effective field theory where the model is a low energy description of a more fundamental theory. In that case one needs to include non-normalizable operators that are suppressed by some high energy scale M. We can think about such operators as emerging from integrating out heavy fields. That is, it is assumed that the "preons" in the new sector interact with the SM fields through "messengers." The messengers are fields that are charged under both the SM and the preon sector, and are assumed to be very heavy, with the mass scale $M \gg \Lambda$. After confining dynamics occur, the couplings between the composite fermions and the SM fields are naturally suppressed by powers of the small ratio Λ/M. In particular, the fact that the coupling between the composite and SM fermions are suppressed makes the composite fermions candidates to be light RH neutrinos.

The work of ref. [5] is a well known example of a model and strong dynamics with unbroken chiral symmetries. The model is based on an $\mathrm{SU}(n+4)_C$ gauge group with a single antisymmetric tensor A and n antifundamentals ψ_f (with $f = 1 \ldots n$). Below the

confinement scale the theory is described by $n(n+1)/2$ massless composite "baryons" $\hat{B}_{ff'} = \hat{B}_{f'f} = \psi_f A \psi_{f'}$. These baryons are identified with the RH neutrinos.

In this work, we focus on the $n = 2$ case, that is a model with a gauge group $\mathrm{SU}(6)_C$. This model has three massless baryons that can give mass to the three SM neutrinos. These baryons are connected to the SM neutrinos through higher dimension operators suppressed by the high mass scale M. The lowest dimension operator of interest is

$$\lambda^{ff',i} \frac{(\psi_f^T A^* \psi_{f'}) L_i^\dagger \tilde{H}}{M^3} \equiv \lambda^{ff',i} \epsilon^3 B_{ff'} L_i^\dagger \tilde{H}, \tag{2.1}$$

where $i = 1, 2, 3$ runs over the three SM generations and we define

$$\epsilon \equiv \frac{\Lambda}{M}, \qquad B_{ff'} \equiv \frac{\psi_f^T A^* \psi_{f'}}{\Lambda^3}, \qquad \tilde{H} \equiv i\sigma^2 H^*, \tag{2.2}$$

such that $B_{ff'}$ are the canonically normalized baryon fields. If lepton number is a good symmetry of the model, the term in (2.1) generates Dirac masses to the SM neutrinos

$$m_\nu = \lambda \epsilon^3 v, \tag{2.3}$$

where v is the Higgs vev and flavor indices are suppressed.

We can also include lepton number violating terms in the theory. Then we have the well known see-saw term

$$y_{ij} \frac{\bar{L}_i \bar{L}_j H H}{M}. \tag{2.4}$$

In addition, there are new terms involving the composite fermions

$$h^{ff',gg'} \frac{(\psi_f A \psi_{f'})(\psi_g A \psi_{g'})}{M^5} = h^{ff',gg'} M \epsilon^6 B_{ff'} B_{gg'}. \tag{2.5}$$

The neutrino mass matrix is now a 6×6 matrix that in the $(L_\alpha, B_{ff'})$ basis is given by

$$\begin{bmatrix} yv^2/M & \lambda \epsilon^3 v \\ \lambda \epsilon^3 v & h \epsilon^6 M \end{bmatrix}, \tag{2.6}$$

where flavor indices are implicit. Diagonalizing the matrix and assuming that all the dimensionless couplings are order one we get

$$m_\nu \sim \frac{v^2}{M}, \qquad m_N \sim \epsilon^6 M, \qquad \theta_{LR} \sim \min\left(\sqrt{\frac{m_\nu}{m_N}}, \sqrt{\frac{m_N}{m_\nu}} \right). \tag{2.7}$$

m_ν and m_N are, respectively, the LH and RH neutrino masses, and θ_{LR} are the mixing angles between the LH and RH neutrinos.

We learn that composite RH neutrinos can naturally give small neutrino masses. They can be Dirac masses, eq. (2.3), or Majorana masses, eq. (2.7).

JHEP12(2008)016

	$SU(6)_C$	$SU(2)_L$	$U(1)_Y$	Q	spin	L	Q_{ps}	$SU(2)_\psi$
${}_iL_L^\alpha$	1	2	$-\frac{1}{2}$	0, -1	$\frac{1}{2}$	1	0	1
${}_iE_R$	1	1	-1	-1	$\frac{1}{2}$	-1	0	1
H^α	1	2	$\frac{1}{2}$	1, 0	0	0	0	1
${}_g\Omega_{ab}^\alpha$	15	2	$-\frac{1}{2}$	0, -1	0	0	2	1
${}_f\psi_a$	6	1	0	0	$\frac{1}{2}$	0	1	2
A_{ab}	15	1	0	0	$\frac{1}{2}$	-1	2	1
Φ_{ab}	15	1	0	0	0	0	2	1
${}_kN$	189 ; 1	1	0	0	$\frac{1}{2}$	break	0	1

Table 1: The fermions and scalars of the $SU(6)_C$ model. We divide the particles into four groups. From top to bottom: the SM fields, the messenger, the preons and the optional lepton number violating Majorana fermion.

3. The UV complete theory

In [3] a low energy effective theory approach was used. In this section, we give UV completions of the models studied in [3]. In III.A, we present the particle content. In III.B, the interactions relating to the new fields are listed and the number of physical parameters is discussed. In III.C, we obtain bounds on the parameters from $\mu \to e\gamma$ and muon-conversion experiments. In appendix. A, we show how the coupling of eqs. (2.1) and (2.5) are obtained by integrating out the heavy fields of the UV complete theory.

3.1 Particle content

We consider the case of an $SU(6)_C$ gauge symmetry in the preon sector. As we mention before, this gives three composite neutrinos. The generalization for models with a larger symmetry is straightforward. The minimum particle content of this model is listed in table 1. In the table we identify representations by their dimension. In the SM sector, ${}_iL_L^\alpha$ and H^α are lepton and Higgs doublets carrying $SU(2)_L$ index $\alpha = 1, 2$ while ${}_iE_R$ is an $SU(2)_L$ singlet. L and E carry generation index $i = 1, 2, 3$.

There are two types of fermions in the preon sector. The first fermion, ${}_f\psi_a$, is a fundamental under $SU(6)_C$ that carries a flavor index $f = 1, 2$ and $SU(6)_C$ index, $a = 1, 2, \ldots, 6$. The other fermion, A_{ab}, is a second rank antisymmetric tensor, that is it belongs to the $(0, 1, 0, 0, 0)$ representation of $SU(6)$. Composite fermions are made of these two types of fundamental fermions.

Aside from the fermions we also need scalars that connect the fermions to the SM fields. One scalar, ${}_g\Omega_{ab}^\alpha$, is a heavy messenger, as it is charged under both the SM and preon gauge groups. It carries a generation index $g = 1, 2$ (as discuss below, this is necessary for LG) and transforms as a second rank antisymmetric tensor under $SU(6)_C$ and as a fundamental under $SU(2)_L$. The other heavy scalar, Φ_{ab}, used for connecting two ψ's together, transforms as a second rank antisymmetric tensor under $SU(6)_C$. The mass scale of both heavy scalars is M, which is assumed to be much larger than the preon confinement scale Λ.

Lastly, in models with lepton number violation we need one more field that breaks lepton number. This field, ${}_kN$, is a SM singlet, and can be either a singlet or a 189 of $\mathrm{SU}(6)_C$. [The 189 of SU(6) is $(0,1,0,1,0)$.] Here $k=1,2$ is the generation index, which is needed, as discuss below, for LG.

There are three accidental symmetries for this model, $\mathrm{U}(1)_L$, $\mathrm{U}(1)_{ps}$, and $\mathrm{SU}(2)_\psi$. $\mathrm{U}(1)_L$ is the SM lepton number L. It is exact in the model without N, but broken when the Majorana field N is included. $\mathrm{U}(1)_{ps}$, where "ps" stands for "preon sector", corresponds to a preon sector charge, Q_{ps}. Only preons and heavy scalars carry such charge. $\mathrm{SU}(2)_\psi$ is a symmetry due to the antisymmetry of the ψ field and correspond to flavor rotation between the two flavors of ψ. Only ψ is charged under this symmetry.

3.2 Interactions

We move to discuss the renormalizable interaction terms of the model. The SM Yukawa interactions

$$Y^e_{ij}\bar{L}^i_L H E^j_R + h.c., \qquad i,j=1,2,3, \tag{3.1}$$

are well known, and we do not discuss them any further. We only recall that the Yukawa couplings, Y^e_{ij}, contain 9 complex parameters.

There are mass terms for the new scalar fields

$$M^2_{\Omega gg'}\Omega^\dagger_g\Omega_{g'} + M^2_\Phi\Phi^\dagger\Phi. \tag{3.2}$$

Here M^2_Φ is a dimensionfull coupling with 1 real parameter, and M^2_Ω is a 2×2 hermitian matrix with 3 real and 1 imaginary parameters. We assume that all new masses are of the same order, $M^2_\Omega \sim M^2_\Phi \sim M^2$.

There are also interaction terms that involve the new fields. In both the L-conserving and L-violating models, the following terms are the most relevant to our study

$$Y^L_{gi}A\Omega^\dagger_g L_i \; + \; h.c., \tag{3.3}$$

$$\tilde{M}_g\tilde{H}^\dagger\Phi^\dagger\Omega_g \; + \; h.c., \tag{3.4}$$

$$Y^A_{ff'}\psi_f\Phi^\dagger\psi_{f'} \; + \; h.c.\,. \tag{3.5}$$

These couplings generate the effective Yukawa interaction of (2.1) via the diagram in figure 1a (see appendix A). The coupling Y^L_{gi} is a general 2×3 matrix containing 6 real and 6 imaginary parameters. $\tilde{M}_g$ corresponds to two dimension full complex coefficients with $g=1,2$. We assume that each of the elements of $\tilde{M}_g$ is of order M. The coupling $Y^A_{ff'}$ is a 2×2 antisymmetric matrix with 1 complex parameter (see appendix A).

In the L-violating case we include the N field. The relevant couplings include a Majorana mass term

$$M_{Nkk'}N_kN_{k'}, \tag{3.6}$$

where we assume $M_N \sim M$, and interaction terms

$$Y^N_k\Phi^\dagger A N_k + h.c.\,. \tag{3.7}$$

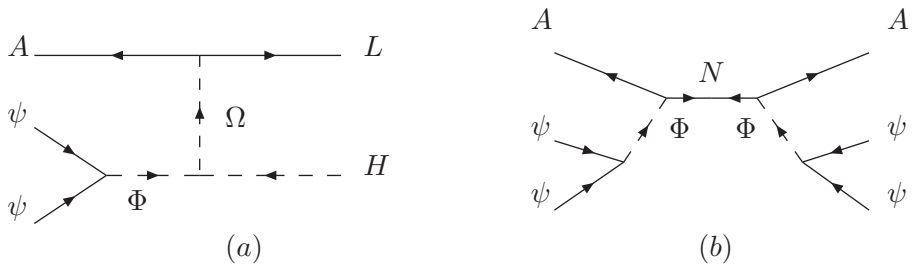

Figure 1: The diagrams that generate the effective couplings of the model. (a) generates the Yukawa coupling of eq. (2.1) and (b) the L-violating term of eq. (2.5).

The mass term (3.6) and the interaction term (3.7) are included for the two possible representations of N, the singlet and the 189. These two terms generate the L-violating term of eq. (2.5) through the diagram in figure 1b. If N is a singlet under all the gauge symmetries, an additional coupling

$$y^N_{ik} H^\dagger L_i N_k + h.c., \tag{3.8}$$

exists. This term is the usual Yukawa coupling in the see-saw mechanism. Together with the mass term of (3.6) it generates the usual see-saw term for the light neutrinos.

Aside from the couplings relating to neutrino masses and LG, there are couplings that connect the new scalars to the SM Higgs field

$$\lambda^{\Omega(1)}_{gg'} H^\dagger \Omega_g H^\dagger \Omega_{g'} + h.c., \qquad \lambda^{\Omega(2)}_{gg'} H^\dagger H \Omega^\dagger_g \Omega_{g'}, \qquad \lambda^\Phi H^\dagger H \Phi^\dagger \Phi. \tag{3.9}$$

These couplings result in having a Higgs mass much above the weak scale unless they are fine-tuned. This is the usual fine tuning problem of the SM. In this work we do not try to solve this problem, we just assume that there is a solution. Thus, in the following we assume that the couplings in (3.9) vanish.

Next we count the number of physical parameters in the various models. In particular, it is important to show that there are CP violating phases in the couplings that we used for LG. We start with the L-conserving model. The parameters of the model discussed above introduced 22 real and 19 imaginary parameters. The counting is summarized in table 2. Not all of these parameters, however, are physical. In order to count the number of physics parameters we need to see how many global symmetries are broken by the new terms. The global symmetry breaking pattern is

$$\mathrm{U}(3)_L \times \mathrm{U}(3)_E \times \mathrm{U}(1)_A \times \mathrm{U}(2)_\psi \times \mathrm{U}(2)_\Omega \times \mathrm{U}(1)_\Phi \to \mathrm{U}(1)_L \times \mathrm{U}(1)_{ps} \times \mathrm{SU}(2)_\psi.$$

Thus, we can eliminate 7 real and 16 imaginary parameters corresponding to the broken generators. This leave us with 15 real and 3 imaginary parameters. It is convenient to work in a basis where all mass parameters are real and diagonal. In that basis the three CPV phases are in Y^L. Note that if we had only one generation for Ω there would be no CPV in the model.

Symbol	Number of parameters (R+I)	Number of Physical parameters (R+I)
M^2_Ω	3+1	2+0
M^2_Φ	1+0	1+0
$\tilde{M}$	2+2	2+0
Y^e	9+9	3+0
Y^L	6+6	6+3
Y^A	1+1	1+0
M_N	3+3	2+0
Y^N	2+2	2+1
y^N	6+6	6+6

Table 2: Parameter counting. We divide the couplings into three groups: For the L-conserving model, we only have the couplings in the first group. For the L-violating model, if N is a 189, we have the couplings in both the first and the second group. When N is a singlet, we have all the three groups. For each coupling we list the number of parameter as well as the number of parameter in our "physical" basis choice. We list separately the number of real and imaginary parameters.

When including the N field there are more parameters and two more broken global symmetries, $\mathrm{U}(2)_N$ and $\mathrm{U}(1)_L$. The global symmetry breaking pattern becomes

$$\mathrm{U}(3)_L \times \mathrm{U}(3)_E \times \mathrm{U}(1)_A \times \mathrm{U}(2)_\psi \times \mathrm{U}(2)_\Omega \times \mathrm{U}(1)_\Phi \times \mathrm{U}(2)_N \to \mathrm{U}(1)_{ps} \times \mathrm{SU}(2)_\psi.$$

We then eliminate 8 real and 20 imaginary parameters corresponding to the broken generators. When N is a 189, there are 19 real and 4 imaginary parameters in the theory. When N is singlet, the model has 25 real and 10 imaginary parameters.

3.3 Experimental bounds

One potential issue with the full model is the contributions of the heavy particles to rare processes. The effect of new SM singlets is quite small as they do not couple to SM fields. The messenger, however, can have significant effect as it charged under the SM gauge group. Here we study the most significant bounds. They arise from $\mu \to e\gamma$, muon electron conversion in nuclei, and cosmology.

Starting with $\mu \to e\gamma$, see figure 3. In the appendix we calculate the decay rate, eq. (B.12),

$$Br(\mu \to \gamma e) = \frac{\alpha |Y^L|^4}{3072\pi G_F^2 M^4} \tag{3.10}$$

Comparing it to the experimental bound [6]

$$Br(\mu \to eX) < 1.2 \times 10^{-11}, \tag{3.11}$$

we obtain a lower bound

$$M > 10|Y^L| \text{ TeV}. \tag{3.12}$$

For coherent muon electron conversion in nuclei (figure 4), the theoretical expression is estimated in the appendix, eq. (C.6),

$$Br(\mu \to e, Ti) \equiv \frac{w_{\rm conv}}{w_{\rm cap}} \approx 10^8 |Y^L|^4 \left(\frac{m_\mu}{M}\right)^4. \tag{3.13}$$

The experimental bound on the branching ratio is [7]

$$Br(\mu \to e) < 1.7 \times 10^{-12}. \tag{3.14}$$

Comparing the theoretical prediction with the experimental data we get a bound on M

$$M > 10 |Y^L| \text{ TeV}. \tag{3.15}$$

which is the same as the one we get from $\mu \to e\gamma$, (3.12).

Aside from the constraints coming from particle physics, constraints from big-bang nucleosynthesis (BBN) can be strong when the RH neutrinos have Dirac masses. The reason for this is that the three extra light modes can be populated before BBN. Then the energy density, which depends on the number of relativistic particles, would be different from the SM one. This difference affects the observed ratio of primordial elements.

The number of light degrees of freedom is parameterized by the number of neutrinos. The most stringent bound coming from BBN and CMB data implies $N_\nu \leq 3.3$ at 95% CL [8], that is, the effective contribution of the RH neutrinos can account for as much as 0.3 of one active neutrino.

This bound rules out any model where the RH neutrinos are populated at the same temperature as the SM ones. Yet, if the temperature of the RH sector is lower, the model is viable. The point is that the contribution to the energy density scales like T^4 (where T is the temperature). Explicitly, the energy density of the SM sector (with temperature $T_{\rm SM}$) and the three light composite neutrinos (with temperature $T_{\rm CN}$) is given by [9]

$$\rho = \frac{\pi^2}{30}\left(g_* T_{\rm SM}^4 + \frac{7}{8} \times 3 \times 2 \times T_{\rm CN}^4 \right), \tag{3.16}$$

where $g_* \simeq 11$ is the effective number of degrees of freedom in the SM sector (including three massless LH neutrinos). Requiring that the RH neutrinos contribute less than 0.3 active neutrinos is equivalent to the condition

$$3T_{\rm CN}^4 \lesssim 0.3 T_{\rm SM}^4 \quad \Rightarrow T_{\rm CN} \lesssim 0.5\, T_{\rm SM}. \tag{3.17}$$

We learn that we need the composite neutrino temperature to be less than about half of the SM one in order to satisfy the energy density constraint from BBN.

Next we compare the temperature of the two sectors. The preon confinement scale, Λ, is larger than the EW scale. Therefore, the light composite neutrinos decouple from the thermal bath at $T \sim \Lambda$ which is before the EW phase transitions. Thus, the temperature of the composite neutrinos is different than that of the active one. The temperatures ratio is inversely proportional to the ratio of scale factors, $T_{\rm CN} = (a_i/a_f)\,\Lambda$. The temperature in the SM sector, however, is not just inversely proportional to the scale factor, but is

higher than this due to the decrease in the number of degrees of freedom. The total number of degrees of freedom in SM sector is $g_* \simeq 106$ when $T = \Lambda$ but becomes $g_* \simeq 11$ when $T = T_{\rm SM}$ just before BBN. Making the conservative assumption that the EW phase transition is of second order and thus gives no latent heat, the equality between the initial and the final entropies in SM sector gives

$$106 \times a_i^3 \times \Lambda^3 = 11 \times a_f^3 \times T_{\rm SM}^3 \;\Rightarrow\; T_{\rm CN} \simeq 0.47\, T_{\rm SM}, \tag{3.18}$$

which satisfies the BBN bound (3.17). When the SM is extended to include extra fields (like in the MSSM) or when the EW phase transition is first order, $T_{\rm CN}/T_{\rm SM}$ is even smaller and thus also satisfies the BBN bound.

4. Leptogenesis

As has been discussed, one phenomenological use of the composite model is the realization of leptogenesis. In this section we discuss two LG possibilities corresponding to different reheating temperatures and particle contents. First, we study a model with L-violating interactions and low reheating temperature, T, that is, $T \ll \Lambda$. In this model, standard LG from decays of the heavy composite RH neutrinos is possible. Second, we study a Lepton number conserving model with $T \gg \Lambda$. We can have a realization of Dirac type LG where the new fields can be as light as 10 TeV.

4.1 Standard leptogenesis

Consider the L-violating model with $T \ll \Lambda$. In this case, the preon sector is in its confining phase, and the effects of the interior structure of the RH neutrinos cannot be probed. The model looks like the standard see-saw model, and thus we should check if we can get standard LG in that case.

Using eq. (2.7), assuming that all dimensionless couplings are $O(1)$, and setting the active neutrino mass to $m_\nu \sim 10^{-2}$ eV, the composite RH neutrino mass is of order

$$m_N \sim 10^{15} \epsilon^6 \text{ GeV}. \tag{4.1}$$

We define the standard two parameters [2]

$$\tilde{m} \equiv 8\pi \frac{v^2}{m_N^2} \Gamma_D, \qquad m_* \equiv 8\pi \frac{v^2}{m_N^2} H\Big|_{T=m_N}. \tag{4.2}$$

They represent the particle decay and the universe expansion rate relating to LG. The baryon asymmetry is estimated [2]

$$Y_{\Delta B} \simeq \frac{135\zeta(3)}{4\pi^4 g_*} \sum_\alpha \varepsilon_{L\alpha\alpha} \times \eta_\alpha \times C \simeq 10^{-3} \times \eta \times \varepsilon_L, \tag{4.3}$$

where α is a flavor index, $g_* \simeq 106$ as in the SM, and η_α is the efficiency factor of LG under various washout effects. In the weak washout regime ($\tilde{m} \ll m_*$), we have $\eta \simeq \tilde{m}^2/m_*^2$, while in the strong washout regime ($\tilde{m} \gg m_*$) we have $\eta \simeq m_*/\tilde{m}$. We use here the SM value,

$C \simeq 12/37$, to characterize the sphaleron effects that convert L-number into B-number. For the sake of simplicity, we ignore flavor effects, as they are not changing the order of magnitude of our results. (For a review of flavor effects see, for example, [2].)

Similar to standard LG, the asymmetry ε_L in this case (with Yukawa coupling $\lambda\epsilon^3$) is given by [10] (with $y_n \equiv M_\beta^2/M_\alpha^2$)

$$\begin{aligned}\varepsilon_{L\alpha\alpha} &\equiv \frac{\Gamma(N_\alpha \to LH) - \Gamma(N_\alpha \to \bar{L}H^*)}{\Gamma(N_\alpha \to LH) + \Gamma(N_\alpha \to \bar{L}H^*)} \\ &= \sum_{\alpha\neq\beta} \frac{\mathcal{I}m[(\lambda\lambda^\dagger)^2_{\alpha\beta}]\epsilon^6}{8\pi(\lambda\lambda^\dagger)_{\alpha\alpha}} \sqrt{y_n}\left[1-(1+y_n)\ln\left(\frac{1+y_n}{y_n}\right)\right] \sim \frac{1}{8\pi}\lambda^2\epsilon^6. \end{aligned} \tag{4.4}$$

Note that we explicitly kept the $O(1)$ coupling λ in order to demonstrate where the CP violating phase arises. Using the neutrino mass condition, (4.1), the RH neutrino decay rate can be written as

$$\Gamma \simeq \frac{\epsilon^6}{8\pi} m_N \sim 10^{-13}\frac{m_N^2}{\mathrm{TeV}}. \tag{4.5}$$

The expansion rate at the time of decay is given by [9]

$$H|_{T=m_N} \simeq 10^{-15}\frac{m_N^2}{\mathrm{TeV}}. \tag{4.6}$$

Since $\Gamma \gg H$, the decay is in the strong washout regime. The baryon asymmetry is therefore

$$Y_{\Delta B} \simeq 10^{-3}\varepsilon_L\left(\frac{H|_{T=m_N}}{\Gamma}\right) \sim 10^{-5}\epsilon^6. \tag{4.7}$$

Comparing to the observed value, $Y_{\Delta B} \simeq 10^{-10}$, we find that the following range of parameters lead to successful leptogenesis:

$$m_N \sim 10^{10}\ \mathrm{GeV}, \qquad \epsilon \sim 10^{-1}, \qquad M \sim 10^{16}\ \mathrm{GeV}, \qquad \Lambda \sim 10^{15}\ \mathrm{GeV}. \tag{4.8}$$

These parameters correspond to a high energy LG scenario which gives the observed values for m_ν and $Y_{\Delta B}$.

4.2 Dirac-type leptogenesis

Next we move to study the $T \gg \Lambda$ case. Then the preons are asymptotically free and we perform all the calculations at the preon level. Since we care only about rough estimates we do not include $\mathrm{SU}(6)_C$ radiative corrections. Here we study the L-conserving model. We get L-number conservation by not including the heavy Majorana fermion N. Below we show that in that case the decay of the heavy messenger Ω gives a realization of Dirac-type LG [11, 12].

The idea is as follows. When $T \sim M$, the decay of Ω and $\bar{\Omega}$ gives different L and $\bar{L}$ in the final state. Yet, the decays also generate exactly the same difference between the number of A and $\bar{A}$. Since L and A carry opposite lepton numbers, the total lepton number is zero. Yet, each sector (L and A) carry finite and opposite lepton number. Since the equilibrating rate is smaller than the expansion rate, the L-number is preserved in each

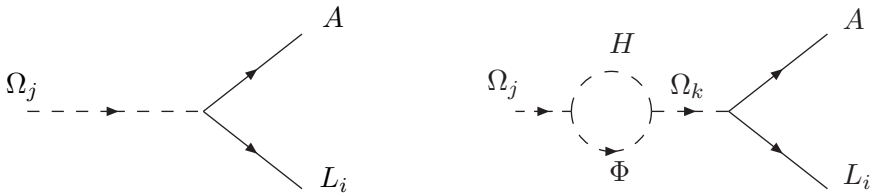

Figure 2: The Ω decay process that gives the L-asymmetry.

sector. When the EW phase transition occurs, sphaleron processes only affects L and $\bar{L}$, but not A and $\bar{A}$. Thus, the sphalerons convert part of the L-number stored in the leptons into B-number. We can end up with positive B-number and negative L-number in SM sector. Since we only observe the B-number of the universe this mechanism can be valid.

Specifically we consider the decay $\Omega \to LA$ (figure 2). The asymmetry between this decay and its conjugate process comes from the interference between the tree level and the one loop diagrams. It is given by

$$\begin{aligned}\epsilon_{\Omega_j} &\equiv \frac{\Gamma(\bar{\Omega}_j \to \bar{A}\bar{L}) - \Gamma(\Omega_j \to AL)}{\Gamma(\bar{\Omega}_j \to \bar{A}\bar{L}) + \Gamma(\Omega_j \to AL)} \\ &= \frac{1}{8\pi}\frac{M_j^2 - M_\Phi^2}{M_j^2 - M_k^2}\left(\frac{\tilde{M}_j\tilde{M}_k}{M_j^2}\right)\frac{\mathcal{I}m((Y^{L\dagger}Y^L)_{jk})}{(Y^{L\dagger}Y^L)_{jj}} \sim \frac{r^2}{8\pi}, \qquad r \equiv \frac{\tilde{M}}{M}. \end{aligned} \tag{4.9}$$

Here $j,k = 1,2$ and $j \neq k$. M_j, M_k, M_Φ are the masses of Ω_i, Ω_j, Φ, and we assume $M_j \sim M_k \sim M_\Phi$ with $M_\Phi < M_j$ such that Φ can be on-shell in the loop. Following the convention in table 2, we take the trilinear coupling, $\tilde{M}$, to be real. The CP phase that contributes to the asymmetry is in Y^L. In half of the parameter space we end up with negative L-number in the SM sector and positive L-number in the preon sector.

The natural scale of $\tilde{M}$ is $\tilde{M} \sim M$, that is $r \sim 1$. (Yet, in the following we investigate the allowed parameter space letting the ratio r to vary.) The main result from eq. (4.9) is that we can get very large lepton asymmetry. Thus, we have to check if washout effects can reduce the asymmetry to the observed level.

There are two kinds of washout processes: inverse decays and scattering that equilibrates the L-number. Here, we would like to demonstrate that we can get Dirac-LG. Thus, we only try to find some parts of the parameters space that can produce the observed value of the asymmetry. We concentrate on the part of the parameter space where the equilibrating scattering is negligible, that is, where the equilibrating rate between positive and negative L-numbers is slower than the expansion of the universe.

The parameter space where equilibrating scattering is negligible can be found as follows. First, when $T < M$ the only equilibrating process in our case is $\bar{A}\bar{L} \to H\bar{\psi}\bar{\psi}$, coming

from the diagram in figure 1. Its interaction rate can be estimated as

$$R_{\rm eq}|_T \sim |Y^A|^2 |Y^L|^2 \left(\frac{\tilde{M}}{M}\right)^2 \frac{T^7}{M^6}. \tag{4.10}$$

Here the M^{-8} factor comes from the masses of virtual Ω and Φ. Unlike the original Dirac LG scenario [11] where $R_{\rm eq} \propto T$, in our case $R_{\rm eq}$ drops much faster than H, that is, $R_{\rm eq} \propto T^2$. Thus, if the equilibrating is slower than the expansion just when Ω begins to decay, that is,

$$R_{\rm eq}|_{T=M} \sim |Y^L|^2 |Y^A|^2 r^2 M < H|_{T=M} \sim 10^{-15} \frac{M^2}{\rm TeV}, \tag{4.11}$$

then the equilibrating rate after this is always smaller than the expansion rate. In that case scattering is very rare and can be neglected. That is, by choosing the parameter space satisfying eq. (4.11), we only need to include the inverse decay for washout effect.

Within this range of parameters we only need to study the effect of inverse decays. The L-asymmetry is given in eq. (4.9). We see that for $r > 10^{-3}$, the inverse decay must be significant in order to reduce the asymmetry into the observed value, $Y_{\Delta B} \sim 10^{-10}$. When including the efficiency factor given by the strong inverse decay, eq. (4.3), we have the asymmetry

$$Y_{\Delta B,\Omega} \simeq 10^{-4} \times r^2 \times \left(\frac{H|_{T=M}}{\Gamma_\Omega}\right) \sim 10^{-18} \times r^2 \times |Y^L|^{-2} \frac{M}{\rm TeV}. \tag{4.12}$$

If the inverse decay lowers the baryon asymmetry to the observed value, $Y_{\Delta B} \sim 10^{-10}$, the following condition should be satisfied

$$r^2 |Y^L|^{-2} \frac{M}{\rm TeV} \sim 10^8. \tag{4.13}$$

We are ready to find a region of the parameter space that gives successful Dirac-LG. Besides the two constraints eqs. (4.11) and (4.13) we also have a constraint from the Dirac neutrino mass

$$m_\nu = \left(\frac{\tilde{M}}{M}\right) |Y^L||Y^A| \epsilon^3 v \sim 10^{-2}\,{\rm eV}. \tag{4.14}$$

We also require $\epsilon \equiv (\Lambda/M) < 10^{-2}$, in order justify integrating out the heavy scalars. Then, eq. (4.14) gives

$$r|Y^L||Y^A| > 10^{-7}. \tag{4.15}$$

Last, we use $|Y^L|, |Y^A| \lesssim 1$ in order for perturbation theory to work. Then, combining eqs. (4.11), (4.13) and (4.15) we find a representative region in the parameter space that gives a successful Dirac-type LG:

$$\begin{aligned} &10^{-3} r < |Y^L| < 1, \qquad |Y^A| < 10^{-4} r^{-2}, \qquad |Y^A| < 1, \qquad M > 10\,{\rm TeV}, \\ &10^{-7} r^{-4}{\rm TeV} < M < 10^7 r^{-2}\,{\rm TeV}, \qquad \epsilon < 10^{-2}. \end{aligned} \tag{4.16}$$

As an example, when $r = 1$, the following parameters give a successful Dirac-LG with strong washout effect

$$|\tilde{M}| = M \qquad M = 10\,\text{TeV} \qquad |Y^L| = 10^{-3} \qquad |Y^A| = 10^{-4} \qquad \epsilon = 10^{-2}. \quad (4.17)$$

When $r = 10^{-3}$, the following parameters give a successful Dirac-LG with weak washout effect

$$|\tilde{M}| = 10^{-3}M \qquad M = 10^8\,\text{TeV} \qquad |Y^L| = 10^{-3} \qquad |Y^A| = 10^{-1} \qquad \epsilon = 10^{-2}. \quad (4.18)$$

We note that when $r > 10^{-2}$, the Ω mass can be as low as 10 TeV, which is, much lighter than the Majorana neutrino mass in the standard LG. The reason that we can get low energy LG is that the Dirac neutrino mass is not directly related to the lepton asymmetry. That is, in the composite model the neutrino mass is suppressed by a factor $(\Lambda/M)^3$. The lepton asymmetry, however, is proportional to r, which is not a very small parameter. In standard LG, on the contrary, both the neutrino mass and the lepton asymmetry are proportional to the Yukawa couplings and thus they cannot be too small.

5. Discussions and conclusions

We investigated models of composite RH neutrinos. First we find several UV completions of the models. These full models are not expected to be unique. They serve as an example that such models can be constructed. Then we moved on to study leptogenesis in these models. We find that such models can naturally give leptogenesis. In particular, we discussed two possibilities corresponding to different temperatures and particle contents. In the lepton number violating model we find that they can give standard LG from RH neutrino decay. In models with lepton number conservation, we find that they can provide a realization of low energy Dirac LG. We conclude that the idea of composite RH neutrino is phenomenologically interesting: it naturally gives small neutrino masses and successful leptogenesis.

Acknowledgments

We thank Josh Berger and Itay Nacshon for helpful discussions. This research is supported by the NSF grant PHY-0355005.

A. Matching the UV theory to the effective theory

In this appendix, we obtain the effective Yukawa and L-violating couplings in eqs. (2.1) and (2.5) by integrating out the heavy fields in eqs. (3.3)–(3.8). This gives the relations between the effective couplings λ, h and those of the full theory.

We start from rewriting eqs. (3.3)–(3.8) keeping all the indices explicitly

$$Y^L_{gi} A_{abm} \sigma^2_{mn} \Omega^{ba\alpha}_g L_{i\alpha n} + h.c., \tag{A.1}$$

$$\tilde{M}_g \tilde{H}^\alpha \Phi^{ab} \Omega_{gba\alpha} + h.c., \tag{A.2}$$

$$Y^A_{ff'} \psi_{fam} \sigma^2_{mn} \Phi^{ab} \psi_{f'bn} + h.c., \tag{A.3}$$

$$Y^N_k \epsilon_{abopqr} \epsilon^{opqrst} \epsilon^{uvwxyz} \Phi^{ab} A_{uvm} \sigma^2_{mn} N_{stwxyz,kn} + h.c., \tag{A.4}$$

$$y^N_{ik} H^\alpha L_{\alpha i} N_k + h.c. \tag{A.5}$$

where here the upper indices represent the hermitian conjugate of the fields. As we can see in eq. (A.3), the antisymmetry in the spinor and the $SU(6)_C$ indices require $Y^A_{ff'}$ to be antisymmetric. The indices here are quite cumbersome, and we write them only when it is necessary in the following calculation.

To obtain the effective Yukawa coupling as an $(\psi A \psi L \tilde{H})$ vertex, we need to integrate out the heavy Ω and Φ fields in figure 1a. The Ω and Φ related couplings, including their mass terms and three vertices in the diagram, is

$$-M^2 \Omega^\dagger \Omega - M^2 \Phi^\dagger \Phi + Y^A \psi \Phi^\dagger \psi + Y^{L\dagger} L^\dagger \Omega A^\dagger + \tilde{M}^\dagger \Omega^\dagger \Phi \tilde{H} + h.c.. \tag{A.6}$$

After integrating Ω and Φ out, and using the convention $|\tilde{M}| = rM$, we obtain

$$\frac{1}{M^3} [Y^{L\dagger} r Y^A (L^\dagger A^\dagger \tilde{H})(\psi^T \psi) + h.c.] \tag{A.7}$$

Writing the indices explicitly, we can rearrange the fields into a more transparent form for composite neutrino

$$\begin{aligned} &\frac{Y^{L\dagger}_i r Y^A_{ff'}}{M^3} (L^{*\alpha}_{im} \sigma^2_{mn} A^{*ab}_n \tilde{H}_\alpha)(\psi_{fas} \sigma^2_{st} \psi_{f'bt}) + h.c. \\ &\qquad = \frac{Y^{L\dagger}_i r Y^A_{ff'}}{M^3} (\psi_{fas} \sigma^2_{st} A^{*ab}_m \psi_{f'bt}) \sigma^2_{mn} L^{*\alpha}_{in} \tilde{H}_\alpha + h.c. \\ &\qquad \equiv \lambda^{ff',i} \frac{(\psi^T_f A^* \psi_{f'}) L^\dagger_i \tilde{H}}{M^3} + h.c., \end{aligned} \tag{A.8}$$

where

$$\lambda^{ff',i} = Y^{L\dagger}_i r Y^A_{ff'} \Rightarrow \lambda \sim r |Y^L| |Y^A|. \tag{A.9}$$

Note that the second equality implies that when interchanging ff', the antisymmetry of A^{ab} and $Y^A_{ff'}$ makes the whole RH neutrino part invariant. This gives the correct form for $B_{ff'}$, the massless composite neutrinos.

For the L-violating coupling, eq. (2.5), we need to include the heavy Majorana fermion N. The related couplings in figure 1b are:

$$-MNN - M^2 \Phi^\dagger \Phi + Y^{N\dagger} N^\dagger A^\dagger \Phi A + Y^A \psi \Phi^\dagger \psi + h.c.. \tag{A.10}$$

After integrating out N and Φ, we obtain

$$\frac{(Y^A Y^{N\dagger})^2}{4M^5} (\psi^T \psi A^*)(A^\dagger \psi^T \psi) + h.c.. \tag{A.11}$$

Writing this in a form that is best for studying composite neutrinos, we have

$$\begin{aligned}
&\frac{(Y^A_{ff'}Y^{N\dagger})(Y^A_{gg'}Y^{N\dagger})}{4M^5}(\psi_{fm}\sigma^2_{mn}\psi_{f'n}A^\dagger_o)\sigma^2_{op}(A^*_p\psi_{gs}\sigma^2_{st}\psi_{g't}) \\
&\quad = \frac{(Y^A_{ff'}Y^{N\dagger})(Y^A_{gg'}Y^{N\dagger})}{4M^5}(\psi_{fm}\sigma^2_{mn}A^\dagger_o\psi_{f'n})^T\sigma^2_{op}(\psi_{gs}\sigma^2_{st}A^*_p\psi_{g't}) \\
&\quad \equiv h^{ff',gg'}\frac{(\psi^T_f A^\dagger\psi_{f'})(\psi^T_g A^*\psi_{g'})}{M^5},
\end{aligned} \tag{A.12}$$

where

$$h^{ff',gg'} = \frac{1}{4}(Y^A_{ff'}Y^{N\dagger})(Y^A_{gg'}Y^{N\dagger}) \quad \Rightarrow \quad h \sim |Y^N|^2|Y^A|^2. \tag{A.13}$$

B. Calculation of $\mu \to e\gamma$

In this appendix, we calculate the bounds on M given by the lepton flavor violating (LFV) process $\mu \to e\gamma$. The vertices and the kinematics of the LFV process are shown in figure 3.

Throughout the calculation, we neglect the mass of the out-going electron. We first evaluate the amplitude of the diagram where the photon coming from the external muon. This diagram scales as the electron mass and thus vanish in the limit of massless electron.

Explicitly the diagram gives

$$\begin{aligned}
M_{\mu\to\gamma} &= \bar{u}_{e_R}(-iY^*_L)\int\frac{d^4k}{(2\pi)^4}\frac{i}{k^2-M^2}\frac{i(\not{p}'-\not{k})}{(p'-k)^2}(iY_L)\frac{i(\not{p}'+m_\mu)}{(p'^2-m^2_\mu)}(-ie\not{\varepsilon})u_\mu \\
&= -e|Y^L|^2\bar{u}_{e_R}\left[\int\frac{d^4k}{(2\pi)^4}\frac{\not{p}'-\not{k}}{(k^2-M^2)(p'-k)^2}\right]\frac{\not{p}'+m_\mu}{p'^2-m^2_\mu}\not{\varepsilon}u_\mu.
\end{aligned} \tag{B.1}$$

Here M, m_μ, m_e are the masses of Ω, μ, e, we use $p' \equiv (p-q)$, and ε^μ is the polarization of the outgoing photon. Integrating out the loop momentum and doing the dimensional regularization, we get the amplitude as

$$M_{\mu\to\gamma} = \frac{-ie|Y^L|^2}{32\pi^2}\bar{u}_{e_R}\left(\not{p}'\frac{\not{p}'+m_\mu}{p'^2-m^2_\mu}\not{\varepsilon}\right)\left(\frac{2}{\epsilon}-\gamma+\ln(4\pi)+\frac{1}{2}-\ln M^2\right)u_\mu. \tag{B.2}$$

Here γ is the Euler-Mascheroni constant, $\epsilon \equiv 4-d$ and we take $d \to 4$ for the finite terms. We use the condition of transverse polarization

$$\varepsilon_\mu q^\mu = 0, \qquad \varepsilon_\mu p^\mu = 0, \qquad \varepsilon_\mu p'^\mu = 0. \tag{B.3}$$

Then, we see that the diagram vanishes, that is, $M_{\mu\to\gamma} = 0$.

The amplitude of the diagram where the external photon is emitted by the electron can be written as

$$\begin{aligned}
M_{e\to\gamma} &= \bar{u}_{e_R}(-ie\not{\varepsilon})\frac{i(\not{p})}{(p^2)}(-iY^*_L)\int\frac{d^4k}{(2\pi)^4}\frac{i}{k^2-M^2}\frac{i(\not{p}-\not{k})}{(p-k)^2}(iY_L)u_\mu \\
&= -e|Y^L|^2\bar{u}_e\not{\varepsilon}\frac{\not{p}}{p^2}\left[\int\frac{d^4k}{(2\pi)^4}\frac{\not{p}-\not{k}}{(k^2-M^2)(p-k)^2}\right]u_\mu.
\end{aligned} \tag{B.4}$$

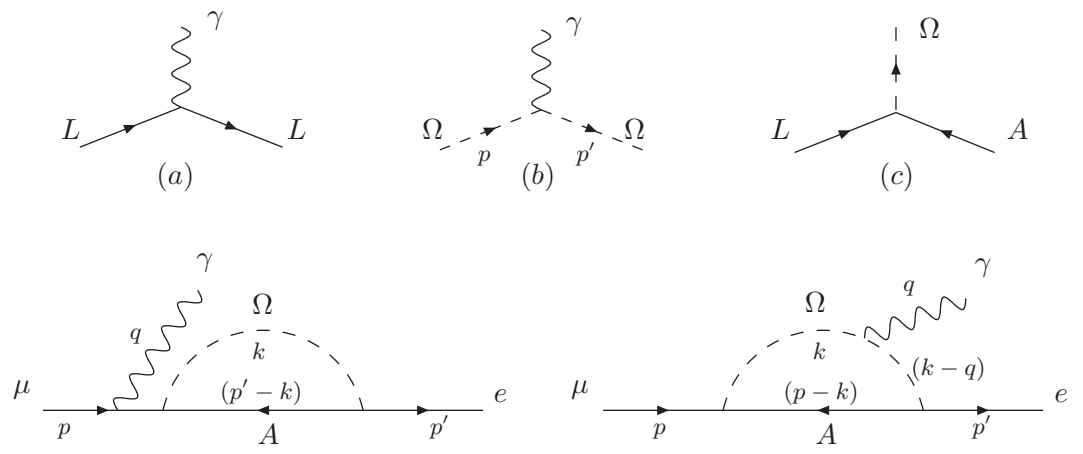

Figure 3: In the upper part are the vertices we use in the calculation: (a) $-ie\gamma^\mu$ (b) $-ie(p+p')^\mu$ (c) iY^L. The lower part are the kinematics we use in the calculation. The case with the photon going out from e is not shown, since we can obtain the result directly from the first diagram.

Integrating out the loop momentum and doing the regularization, this gives

$$\begin{aligned} M_{e\to\gamma} &= \frac{-ie|Y^L|^2}{32\pi^2}\bar{u}_{e_R}\not{\varepsilon}\left(\frac{\not{p}'}{m_\mu^2}\not{p}'\right)\left[\frac{2}{\epsilon}-\gamma+\ln(4\pi)+\frac{1}{2}-\ln M^2+\frac{1}{3}\left(\frac{m_\mu}{M}\right)^2\right]u_\mu \\ &= \frac{-ie|Y^L|^2}{32\pi^2}\left[\frac{2}{\epsilon}-\gamma+\ln(4\pi)+\frac{1}{2}-\ln M^2+\frac{1}{3}\left(\frac{m_\mu}{M}\right)^2\right]\varepsilon_\nu\bar{u}_{e_R}\gamma^\nu u_{\mu_R}. \end{aligned} \tag{B.5}$$

when keeping terms up to order $O(m_\mu^2/M^2)$.

For the case with the photon coming out from the internal Ω (see figure 3), the amplitude is

$$\begin{aligned} M_{\Omega\to\gamma} &= \bar{u}_{e_R}(-iY_L^*)\varepsilon_\nu\int\frac{d^4k}{(2\pi)^4}\frac{i}{(k-q)^2-M^2}(-ie(2k-q)^\nu)\frac{i}{(k^2-M^2)}\frac{i(\not{p}'-\not{k})}{(p-k)^2}(iY_L)u_\mu \\ &= -e|Y^L|^2\varepsilon_\nu\bar{u}_{e_R}\left[\int\frac{d^4k}{(2\pi)^4}\frac{(2k-q)^\nu(\not{p}'-\not{k})}{((k-q)^2-M^2)(k^2-M^2)(p-k)^2}\right]u_\mu. \end{aligned} \tag{B.6}$$

Integrating out the loop momentum, taking $m_e = 0$ and using the transverse polarization condition, eq. (B.3), we get the amplitude when keeping the terms up to $O(\frac{m_\mu^2}{M^2})$

$$M_{\Omega\to\gamma} = \frac{ie|Y^L|^2}{32\pi^2}\left[\frac{2}{\epsilon}-\gamma+\ln(4\pi)+\frac{1}{2}-\ln M^2+\frac{1}{6}\left(\frac{m_\mu}{M}\right)^2\right]\varepsilon_\nu\bar{u}_{e_R}\gamma^\nu u_{\mu_R}. \tag{B.7}$$

Combining the three diagrams, we have

$$M_{\mu\to e\gamma} = -\frac{ie|Y^L|^2}{192\pi^2}\left(\frac{m_\mu}{M}\right)^2\bar{u}_{e_R}\not{\varepsilon}u_{\mu_R}. \tag{B.8}$$

Using $m_e = 0$ and eq. (B.3), we can write the result into the well known dipole operator

$$\frac{ie|Y^L|^2}{768\pi^2}\left(\frac{m_\mu}{M^2}\right)\bar{e}_R\sigma_{\mu\nu}F^{\mu\nu}\mu_L. \tag{B.9}$$

JHEP12(2008)016

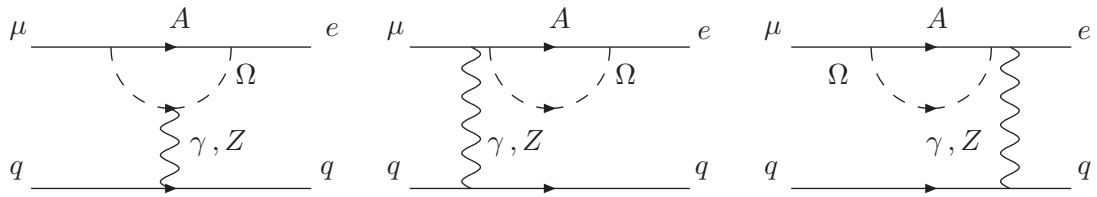

Figure 4: $\mu - e$ conversion in nuclei emitted by photon and Z.

Averaging the incoming muon spin, the amplitude square becomes

$$< |M|^2 >_{\text{spin}} = -\frac{e^2|Y^L|^4}{2\times 192^2\pi^4}(\frac{m_\mu}{M})^4 Tr[\not{p}_e\gamma^\mu(\not{p}_\mu)\gamma_\mu] = \frac{\alpha|Y^L|^4}{96^2\pi^3}\left(\frac{m_\mu^6}{M^4}\right). \tag{B.10}$$

This gives the decay rate

$$\Gamma(\mu\to\gamma e) = \frac{1}{32\pi^2} < |M|^2 >_{\text{spin}} \frac{|q|}{m_\mu^2}\int d\Omega = \frac{\alpha|Y^L|^4}{768^2\pi^4}\frac{m_\mu^5}{M^4}. \tag{B.11}$$

Comparing to the total muon decay rate $\frac{G_F^2 m_\mu^5}{192\pi^3}$, this gives the branching ratio

$$Br(\mu\to\gamma e) = \frac{\alpha|Y^L|^4}{3072\pi G_F^2 M^4}. \tag{B.12}$$

Comparing to the LFV bound today $Br(\mu\to eX) < 10^{-11}$ [6], we have

$$M > 10|Y^L|\,\text{TeV}. \tag{B.13}$$

C. Coherent muon-electron conversion

In this appendix we estimate the bounds from the LFV process of coherent muon-electron conversion (figure 4). For a review of the coherent conversion and how it can be used to put bounds on new physics, see [13, 14] for example.

Our goal is to find the bound on M by comparing the theoretical expression with experimental data. Here we use the general result derived in [13] for the theoretical branching ratio. The low energy effective Hamiltonian is [13]

$$\begin{aligned} H &= -\bar{e}\tilde{O}\mu + h.c. \\ \tilde{O} &= -\sqrt{4\pi\alpha}\left[\gamma_\alpha(f_{E0}-f_{M0}\gamma_5)\frac{q^2}{m_\mu^2} + i\sigma_{\alpha\beta}\frac{q^\beta}{m_\mu}(f_{M_1}+f_{E1}\gamma_5)\right]A^\alpha(q) + \frac{G_F}{\sqrt{2}}\gamma_\alpha(a-b\gamma_5)J^\alpha \\ J^\alpha &= \bar{u}\gamma^\alpha u + c_d\bar{d}\gamma^\alpha d \end{aligned} \tag{C.1}$$

and the final result of the conversion rate is

$$\begin{aligned} w_{\rm conv} &= 3\times 10^{23}(w^{(1)}_{\rm conv}+w^{(2)}_{\rm conv})\,{\rm sec}^{-1},\\ w^{(1)}_{\rm conv} &= \left| f_{E0}I_p - \frac{G_F}{\sqrt{2}}\frac{m_\mu^2}{4\pi Z\alpha}a(Z(2+c_d)I_p+N(1+2c_d)I_n)+f_{M1}I_{34}\right|^2,\\ w^{(2)}_{\rm conv} &= \left| f_{M0}I_p - \frac{G_F}{\sqrt{2}}\frac{m_\mu^2}{4\pi Z\alpha}b(Z(2+c_d)I_p+N(1+2c_d)I_n)+f_{E1}I_{34}\right|^2, \end{aligned} \tag{C.2}$$

where

$$I_p=-(I_1^p+I_2^p),\qquad I_n=-(I_1^n+I_2^n),\qquad I_{34}=I_3+I_4. \tag{C.3}$$

Here q represents the photon momentum, and the terms containing A^α in the Hamiltonian describe the transition that is mediated by a photon. The I's in the last part are coefficients for various elements including the proton-neutron distribution function and the EM field inside the nucleus. They have been calculated in [14] for various materials.

We are ready to use these results in the composite model. The rate of $\mu N\to eN$ arising from the preon sector is given by the six diagrams in figure 4. Doing the same calculation as in appendix B but allowing the out-going photon to be off-shell, the coefficients in eq. (C.1) are of order

$$f_{E0}\sim -f_{M0}\sim f_{M_1}\sim -f_{E_1}\sim a\sim b\sim \frac{|Y^L|^2}{768\pi^2}\frac{m_\mu^2}{M^2},\qquad c_d\sim 1. \tag{C.4}$$

Given these coefficients and the I's calculated in [13, 14] (which are of order $10^{-1}\,{\rm GeV}^{-\frac{1}{2}}$), the conversion rate with target ${}^{48}_{22}Ti$ can be estimated as:

$$w_{\rm conv}\sim 10^{14}|Y^L|^4\left(\frac{m_\mu}{M}\right)^4{\rm sec}^{-1}. \tag{C.5}$$

Comparing to the experimental total muon capture rate $w(Ti)_{\rm cap}=2.6\times 10^6\ {\rm sec}^{-1}$ [15], this gives the branching ratio of the conversion as

$$Br(\mu\to e,Ti)\equiv\frac{w_{\rm conv}}{w_{\rm cap}}=10^8|Y^L|^4\left(\frac{m_\mu}{M}\right)^4. \tag{C.6}$$

Comparing to the experimental limit $Br(\mu\to e)<1.7\times 10^{-12}$ [7], this gives

$$M>10|Y^L|\,{\rm TeV}. \tag{C.7}$$

References

[1] M. Fukugita and T. Yanagida, *Baryogenesis without grand unification*, *Phys. Lett.* **B 174** (1986) 45.

[2] S. Davidson, E. Nardi and Y. Nir, *Leptogenesis*, *Phys. Rept.* **466** (2008) 105 [arXiv:0802.2962].

[3] N. Arkani-Hamed and Y. Grossman, *Light active and sterile neutrinos from compositeness*, *Phys. Lett.* **B 459** (1999) 179 [hep-ph/9806223].

[4] T. Okui, *Searching for composite neutrinos in the cosmic microwave background*, *JHEP* **09** (2005) 017 [hep-ph/0405083].

[5] S. Dimopoulos, S. Raby and L. Susskind, *Light composite fermions*, *Nucl. Phys.* **B 173** (1980) 208.

[6] Particle Data Group collaboration, C. Amsler et al., *Review of particle physics*, *Phys. Lett.* **B 667** (2008) 1.

[7] SINDRUM II collaboration, J. Kaulard et al., *Improved limit on the branching ratio of $\mu^- \to e^+$ conversion on titanium*, *Phys. Lett.* **B 422** (1998) 334.

[8] R.H. Cyburt, B.D. Fields, K.A. Olive and E. Skillman, *New BBN limits on Physics Beyond the Standard Model from He4*, *Astropart. Phys.* **23** (2005) 313 [astro-ph/0408033];
U. Seljak, A. Slosar and P. McDonald, *Cosmological parameters from combining the Lyman-alpha forest with CMB, galaxy clustering and SN constraints*, *JCAP* **10** (2006) 014 [astro-ph/0604335];
WMAP collaboration, J. Dunkley et al., *Five-year Wilkinson Microwave Anisotropy Probe (WMAP) observations: likelihoods and parameters from the WMAP data*, arXiv:0803.0586.

[9] E.W. Kolb and M.S. Turner, *The early universe*, *Front. Phys.* **69** (1990) 1;
S. Dodelson, *Modern cosmology*, Academic Press, Amsterdam The Netherlands (2003), pag. 440.

[10] L. Covi, E. Roulet and F. Vissani, *CP violating decays in leptogenesis scenarios*, *Phys. Lett.* **B 384** (1996) 169 [hep-ph/9605319].

[11] K. Dick, M. Lindner, M. Ratz and D. Wright, *Leptogenesis with Dirac neutrinos*, *Phys. Rev. Lett.* **84** (2000) 4039 [hep-ph/9907562].

[12] H. Murayama and A. Pierce, *Realistic Dirac leptogenesis*, *Phys. Rev. Lett.* **89** (2002) 271601 [hep-ph/0206177].

[13] A. Czarnecki, W.J. Marciano and K. Melnikov, *Coherent muon electron conversion in muonic atoms*, *AIP Conf. Proc.* **435** (1998) 409 [hep-ph/9801218].

[14] R. Kitano, M. Koike and Y. Okada, *Detailed calculation of lepton flavor violating muon electron conversion rate for various nuclei*, *Phys. Rev.* **D 66** (2002) 096002 [*Erratum ibid.* **76** (2007) 059902] [hep-ph/0203110].

[15] T. Suzuki, D.F. Measday and J.P. Roalsvig, *Total nuclear capture rates for negative muons*, *Phys. Rev.* **C 35** (1987) 2212.

JHEP12(2008)016